NASA TN D-71

TECHNICAL NOTE

D-71

AN APPROXIMATE METHOD FOR CALCULATING SURFACE PRESSURES ON CURVED PROFILE BLUNT PLATES IN HYPERSONIC FLOW

By Marcus O. Creager

Ames Research Center
Moffett Field, Calif.

NATIONAL AERONAUTICS AND SPACE ADMINISTRATION

WASHINGTON September 1959

NATIONAL AERONAUTICS AND SPACE ADMINISTRATION

TECHNICAL NOTE D-71

AN APPROXIMATE METHOD FOR CALCULATING SURFACE PRESSURES ON CURVED PROFILE BLUNT PLATES IN HYPERSONIC FLOW

By Marcus O. Creager

SUMMARY

The effects of profile curvature on the flow over blunt plates was investigated. A method of calculating surface pressures was developed which utilized a combination of viscous and inviscid hypersonic parameters. The method was assessed by comparison to experiment conducted in air and helium over a range of Mach numbers from 4 to 13.3 and leading-edge Reynolds numbers from 6,600 to 129,000 for elliptic and circular leading edges.

The favorable comparison between theory and experiment indicates that the prediction scheme developed herein may be used to estimate the complete pressure distribution over blunt plates, including regions close to the stagnation point.

INTRODUCTION

Various theories have been applied to calculate the chordwise pressure distribution for a complete wing in the hypersonic flow regime. Modified Newtonian impact theory has been used (ref. 1) in the stagnation region where the surface inclination to the free stream is large. This method has also been matched with Prandtl-Meyer expansion theory near the sonic point in attempts to predict pressure aft of the sonic point, where the local surface inclination approaches zero. However, these methods are useful for calculation of pressures only in the immediate vicinity of the blunt leading edge of a hypersonic wing for small angle of attack. Linear methods based on viscous boundary-layer and inviscid blast-wave theory were shown in references 2, 3, and 4 to predict the high pressures observed in the region aft of the leading edge along a blunt flat plate for small angles of attack. The reference pressure for these methods was calculated from oblique shock-wave theory, that is, wedge theory. Extension of these linear methods to locations on profiles where large surface inclination is encountered is not feasible within the framework of the oblique shock-wave theory.

The present study was conducted to obtain a useful method of predicting the surface pressures over a blunt curved-profile wing. The results of the present tests of flat plates with elliptic leading edges and the results from similar tests performed elsewhere (refs. 1, 2, 3, 5, and 6) are used to assess the prediction scheme. The present tests were conducted in the Ames 8-inch low density wind tunnel.

SYMBOLS

a_∞ sound speed

a_1, a_2 semimajor and semiminor axis of ellipse (sketch (a))

A constant defined as $\frac{1}{\sqrt{C_W}}$

b_δ factor defined as $\left[\frac{0.865}{M_\delta^2}\frac{T_W}{T_\delta} + 0.166(\gamma-1)\right]\gamma$

b_∞ factor defined as $\left[\frac{0.865}{M_\infty^2}\frac{T_W}{T_\infty} + 0.166(\gamma-1)\right]\gamma$

B empirical constant (see eq. (6))

c $C_\gamma(C_D)^{2/3}$

C_D pressure drag coefficient based on plate thickness and unit width

C_W constant in linear viscosity relation, $\frac{\mu_W}{\mu} = C_W\frac{T_W}{T}$

C_γ constant equal to 0.112 for air and 0.169 for helium

d plate thickness or leading-edge thickness

D pressure drag in free-stream direction

I plane blast-wave parameter, $\frac{M_\infty^2}{\left(\frac{x+\Delta}{d}\right)^{2/3}}$

K_1 factor defined in equation (8)

K_δ factor defined in equation (1)

M_δ local Mach number at the boundary-layer edge

M_∞ free-stream Mach number

p surface pressure

p_α pressure calculated by equation (5)

p_β pressure calculated by equation (6)

$p_{\alpha\beta}$ total inviscid pressure calculated from inviscid theories (see eq. (3))

p_∞ undisturbed free-stream pressure

R shock-wave coordinate (sketch (a))

$Re_{\delta s}$ Reynolds number, $\frac{\rho_\delta u_\delta s}{\mu_\delta}$

$Re_{\infty d}$ Reynolds number, $\frac{\rho_\infty u_\infty d}{\mu_\infty}$

$Re_{\infty s}$ Reynolds number, $\frac{\rho_\infty u_\infty s}{\mu_\infty}$

s surface distance from stagnation point (sketch (a))

T_W wall or plate temperature

T_δ local static temperature at boundary-layer edge

T_∞ free-stream static temperature

u velocity

x chordwise distance from leading edge (sketch (a))

α local surface inclination to free-stream direction, deg

$\bar{\alpha}$ angle of attack of reference plane (sketch (a)), deg

γ ratio of specific heats

Δ detachment distance of bow shock wave (sketch (a))

λ ratio of $\frac{a_1}{a_2}$

μ viscosity

ρ density

$\bar{\chi}_\infty$ hypersonic interaction parameter, $\frac{M_\infty^3 \sqrt{C_W}}{\sqrt{Re_{\infty s}}}$

METHOD OF CALCULATION

Flow Model

The theoretical flow model used to describe the effect of profile curvature on the hypersonic flow over a blunt plate is shown in sketch (a).

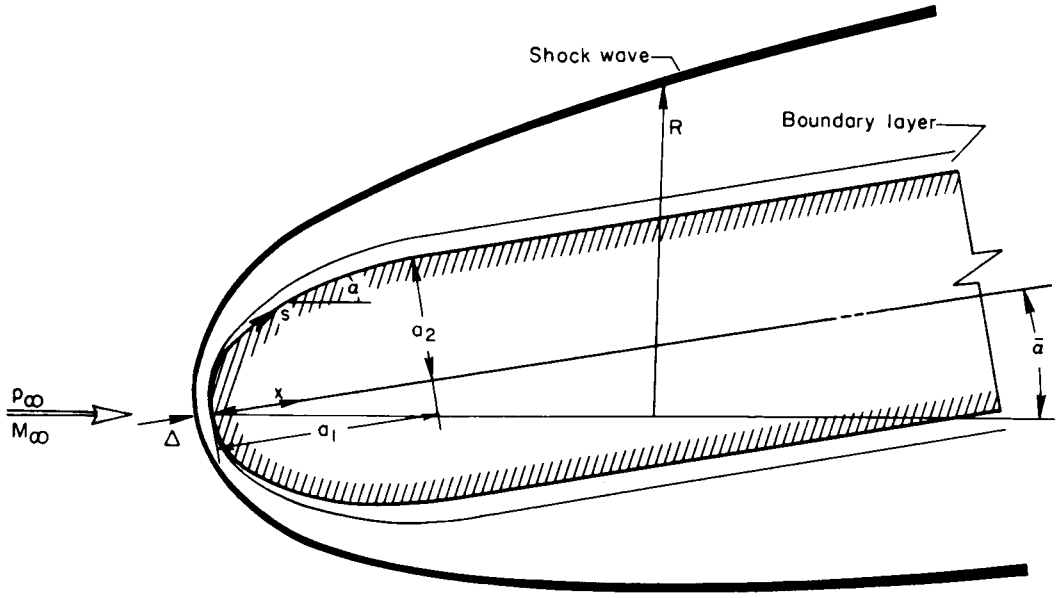

Sketch (a)

The bow shock wave is assumed to be detached. The flow field is assumed to be comprised of a viscous boundary layer near the surface of the body and an inviscid region between the boundary layer and the bow wave.

The displacement effect of the boundary layer is assumed to be a perturbing influence on the inviscid flow field. Hammitt has shown in reference 7 that this assumption is justified, provided the inviscid pressure can be assessed. This perturbation may be expressed as follows,

$$\frac{p}{p_{\alpha\beta}} = 1 + K_\delta A b_\infty \bar{X}_\infty \tag{1}$$

where

$$K_\delta = \frac{b_\delta}{b_\infty}\left(\frac{M_\delta}{M_\infty}\right)^3 \sqrt{\frac{Re_{\infty s}}{Re_{\delta s}}}$$

The subscript δ refers to local conditions at the boundary-layer edge. If one introduces the inviscid pressure ratio $p_{\alpha\beta}/p_\infty$, then equation (1) may be written as

$$\frac{p}{p_\infty} = \frac{p_{\alpha\beta}}{p_\infty}\left(1+K_\delta A b_\infty \bar{X}_\infty\right) \tag{2}$$

From previous results (refs. 2, 3, 4, and 7) it is believed reasonable to assume that the inviscid pressure may be expressed by a sum of two terms, one from shock-wave shape (blast-wave analogy) and one from surface inclination. Thus, the assumption is made that

$$\frac{p_{\alpha\beta}}{p_\infty} = \frac{p_\alpha}{p_\infty} + \frac{p_\beta}{p_\infty} \tag{3}$$

If equation (3) is combined with equation (2) the following equation[1] is obtained

---

[1]The linear method of reference 4 is essentially a linearization of equation (4), wherein the product of the viscous factor $K_\delta A b_\infty \bar{X}_\infty$ and the shock-wave shape term p_ρ/p_∞ is neglected and conditions at the boundary-layer edge are calculated from inviscid sharp-wedge theory.

$$\frac{p}{p_\infty} = \frac{p_\alpha}{p_\infty} + \left(\frac{p_\alpha}{p_\infty} + \frac{p_\beta}{p_\infty}\right) K_\delta A b_\infty \bar{\chi}_\infty + \frac{p_\beta}{p_\infty} \tag{4}$$

This formulation will be used as the basis for the development of a method of calculation for surface pressures wherein the range of surface inclination due to profile curvature is not limited to small angles.

Inviscid Pressure Terms

The portion p_α of the inviscid pressure $p_{\alpha\beta}$ is postulated to depend on the surface inclination. It will be obtained from modified Newtonian impact theory for compression as expressed by

$$\frac{p_\alpha}{p_\infty} = 1 + 1.8\,\frac{\gamma}{2} M_\infty^2 \sin^2\alpha\,, \qquad \alpha > 0 \tag{5}$$

For expansion (negative α) inclinations, the values of p_α will be obtained from Prandtl-Meyer expansion theory starting with the local Mach number at $\alpha = 0$.

The blast-wave theory has been utilized to express the contribution to the surface pressures which arise because of shock-wave shape. Thus, the assumption is made here that

$$\frac{p_\beta}{p_\infty} = BcI = BC_\gamma \left[\frac{C_D}{(x+\Delta)/d}\right]^{2/3} M_\infty^2 \tag{6}$$

The constant C_γ in the blast-wave term will be taken as 0.112 for air and 0.169 for helium. The factor B will be considered as an empirical constant and will be discussed later in more detail. This equation has been applied previously (refs. 2, 3, and 4) to positions aft of a blunt leading edge where the energy of the transverse flow field was constant and represented by the pressure drag of the leading edge. In the region of profile curvature, such as the nose portion of the blunt plate of sketch (a), the energy of the transverse flow field changes because the pressure drag changes with x distance. This variation of energy with

x distance should be introduced into the basic equations of the blast-wave theory and the solution obtained for this new condition.[2] However, for simplicity this variation in drag will be included here by considering the drag coefficient, C_D, in equation (6) as a variable with x distance. The following equation can be used to calculate the variable drag coefficient.

$$C_D = \frac{1}{\frac{\gamma}{2} p_\infty M_\infty \frac{d}{2}} \int_0^x p \tan \alpha \, dx \qquad (7)$$

Viscous Displacement Terms

Local flow properties at the boundary-layer edge will be used to calculate the viscous parameter $(K_\delta A b_\infty \bar{X}_\infty)$. The factor $(A b_\infty \bar{X}_\infty)$ is the familiar hypersonic interaction parameter as calculated from free-stream conditions. The factor K_δ, as may be noted in equation (1), converts the interaction parameter from free-stream to local conditions. Thus, attention is focused on K_δ. The local Mach number, the local Reynolds number, and the constant b_δ depend on values of the total pressure, total temperature, and static pressure at the boundary-layer edge. The local total pressure must be assessed from the meager knowledge available. For this investigation the local total pressure will be assumed to be reduced to that value attained aft of the normal portion of the bow shock wave (ref. 4). The local static pressure will be assumed to be, to first approximation, the inviscid pressure calculable by equation (3) in combination with equations (5) and (6). The total temperature will be assumed constant and equal to the stagnation temperature of the free stream. The factor A will be assumed, as in references 2 and 4, to be $1/\sqrt{C_W}$.

EXPERIMENT

Two test bodies were constructed with unswept leading edges of elliptic profile (see fig. 1). The major to minor axis ratios were 3 to 1 and 4 to 1. The width of the model was sufficient to span the test

[2]The effect of a variation of energy in the blast-wave theory was analyzed by Rogers in reference 8 for one particular form of energy distribution. His analysis indicated that the pressure dependence on the variation in energy is somewhat more complex than the simple method used here. Refinements such as those obtained in reference 8 may be justified when other aspects of the over-all flow field are better known.

stream. The elliptic leading-edge sections were followed by a flat, or slab-type, afterbody of 4 inches in length.

Pressure orifices were installed in the curved surface of the elliptic leading edge and in the flat surface of the afterbody (see fig. 1). The pressures at these orifices were indicated on a multiple-tube manometer by the same technique as explained more fully in reference 2.

Surface pressures were measured for $\bar{\alpha} = +10^\circ$, 0°, and -10°. The tests were performed in the 8-inch low-density wind tunnel (ref. 4) at a Mach number of 5.7, static pressure of 250 microns of mercury and free-stream Reynolds number of approximately 19,000 per inch.

RESULTS AND DISCUSSION

Present Test Results

The data obtained for the two test bodies having elliptic leading-edge profiles are presented in figure 2 for $\lambda = 3$ and figure 3 for $\lambda = 4$. The surface pressure in ratio to the free-stream pressure is plotted versus chordwise distance from the stagnation point in ratio to the plate thickness. Data are shown for $\bar{\alpha} = +10^\circ$, 0°, and -10°. The pressures are noted to decrease with increase in distance and, at a given x/d, to be increased by compression angle of attack and decreased by expansion angle of attack. The value of the local surface inclination is recorded on the figures for the most forward orifice location for each set of data. The data for points aft of the shoulder location were measured on the flat portion of the model.

Equation (4), as described in the previous section, was used to calculate the solid lines in figures 2 and 3. The values of pressure calculated by this method are noted in figures 2 and 3 to compare favorably with the experimental values obtained for $\bar{\alpha} = +10^\circ$, 0°, and -10° and for λ of 3 and 4.

The surface pressure distribution has been measured at $M_\infty = 3.95$ up to the stagnation point for a transverse cylinder ($\lambda = 1$) alone and for a circularly blunted slab (ref. 2). Both of the tests were conducted at $Re_{\infty d}$ of 6,600. The measured pressures for these two tests are plotted in figure 4. The measured pressures for the cylinder match the values obtained at corresponding locations, $\alpha = 60^\circ$ and $\alpha = 30^\circ$, on the plate leading edge. The dashed curves plotted in figure 4 were calculated from modified Newtonian theory, equation (5), and the solid curve from equation (4) (with $B = (1/2)^{2/3}$). Note that good agreement of theory and experiment was obtained for the entire body from $\alpha = 70^\circ$ ($x/d = 0.017$) on the cylinder to $x/d = 2$ on the flat afterbody. Note also that this result was obtained with a value of $B = (1/2)^{2/3}$ in contrast to the value of

B = 1 found to be successful for the plates with elliptical leading edges ($\lambda = 3$ and $\lambda = 4$). The use of different values of B will be discussed in more detail later.

Results of Similar Tests

Tamaki and Kim, reference 6, obtained surface pressures on a plate with an elliptic leading edge at Mach number 6.4 in a shock-driven wind tunnel at the University of Tokyo. The elliptic axis ratio was 8. This shape represents a blunt leading-edge plate with a relatively long section of curved profile surface aft of the leading edge. The plate was unswept and at zero angle of attack. The surface pressures reported were deduced from interferograms of the flow around the body. Values of experimental pressures (from fig. 5 in ref. 6) are reproduced here in figure 5 as circled data points. For locations between the stagnation point and $x/d = 0.1$, the data compare favorably to the values calculated from the Newtonian theory. For locations aft of $x/d = 0.5$, the data are predicted by the present method.

Bogdonoff and Vas reported in reference 5 results of surface pressure measurements on a plate blunted by an elliptic leading edge of axis ratio $\lambda = 3$. The tests were conducted in helium at a Mach number of 13.3 and leading-edge Reynolds number of 37,300. One set of data from reference 5 is plotted here in figure 6. Values of pressure for these conditions calculated from equation (4) are also presented in figure 6 as the solid line. The comparison of experiment with theory is noted to be as good as that obtained for the present tests.

Another comparison can be made for $\lambda = 1$ by piecing together the results obtained at $M = 6.9$ by Penland (ref. 1) for a circular cylinder transverse to the stream, and by Bertram and Henderson (ref. 3) for a circularly blunted flat plate. The Reynolds number based on the diameter of the simple circular cylinder was slightly lower than the Reynolds number based on the diameter of the circular leading edge of the plate. However, both are sufficiently high so that viscous effects are small in comparison to the inviscid effects. Therefore, these two sets of data may be combined, as plotted in figure 7, and considered as representative of a complete chordwise pressure distribution for a circularly blunted slab. The Newtonian theory may be again noted from figure 7 to be useful for large values of inclination, that is, close to the stagnation point. However, equation (4) with $B = (1/2)^{2/3}$ predicts the pressure distribution over the circular cylinder and the afterbody with reasonable accuracy. This agreement is similar to that found in figure 4 for the data for $M_\infty = 3.95$ and $\lambda = 1$.

Evaluation of B

Two values of the empirical constant B have been used herein to obtain agreement between the calculated and the measured pressures. However, discussion of B is best preceded by evaluation of the relative contribution of the blast-wave pressure term to the surface pressure. The relative importance of the terms of equation (4) varies with the test conditions. To indicate the differences for the sets of data assessed, two sets will be scrutinized here. The various terms of equation (4) have been plotted separately in figure 8 for the $M_\infty = 3.95$, $\lambda = 1$ test conditions (see fig. 4) and in figure 9 for the $M_\infty = 5.7$, $\lambda = 3$, $\bar{\alpha} = 0$ (see fig. 2) test condition. For both test conditions the viscous term contributes less than about 10 percent to the surface pressure. The Newtonian pressure increment, equation (5), and the blast-wave pressure increment, equation (6), are noted to vary somewhat in their relative contribution to the surface pressures. The Newtonian pressure increment predominates where α is greater than about 30° for the circular leading-edge region, figure 8. In the region of the shoulder ($\alpha \approx 0$) the blast-wave increment is of major importance. Aft of the shoulder region the contributions of the blast-wave increment fall below the Newtonian increment. The calculated values for the elliptical leading-edge plate are plotted in figure 9. The values of surface inclinations are from $\alpha = 24^\circ$ to $\alpha = 0^\circ$. The calculations are extended back on the afterbody to $x/d = 5$. The values of pressure increments for the elliptical leading-edge plate are similar to those shown in figure 8 for the shoulder region of a circular leading-edge plate. The contribution of the blast-wave increment in this region is large and noted to be different in magnitude for the two bodies. These comparisons emphasize the need for a systematic investigation of the variation of B as obtained from the blast-wave analogy.

The increment p_β/p_∞ of the inviscid pressure ratio was obtained from the analogy of the blast-wave theory to the hypersonic inviscid flow field. This development or analogy is briefly discussed in the appendix, wherein the constant B of equation (6) was calculated from equation (A12) to be 1.07 for air and 1.14 for helium. These values of B are qualitatively substantiated by the experimental results for the elliptical leading-edge plates. The blast-wave analogy does not provide for the value of $B = (1/2)^{2/3}$ which was used for the circular leading-edge plates.

Further assessment of the blast-wave analogy can be made by comparison of predicted shock-wave shapes to measured shock shapes. The shape of the shock wave is given by equation (A12) for a planar body as

$$\frac{R}{d} = K_1 (C_D)^{1/3} \left(\frac{x+\Delta}{d} \right)^{2/3} \tag{8}$$

where K_1 is 0.78 for air and 0.98 for helium. Measured shock-wave coordinates are available for only three sets of the data discussed in the pressure distribution section. Shock-wave coordinates were reported in reference 2 for the circularly blunted flat plates at a Mach number of 3.95 in air. Coordinates of the shock wave over elliptical leading-edge plates were obtained from interferograms published in reference 5 for a Mach number of 13.3 in helium, and in reference 6 for a Mach number of 6.4 in air. These three sets of data are plotted in figure 10, and the values calculated by equation (8) are presented as solid lines. In equation (8) the values of C_D corresponding to the surface pressure calculation were used. The factor K_1 was found to be about 1.2 for the elliptical leading-edge plates for both air and helium, and about 1.5 for the circular leading-edge plate in air. The values of K_1 obtained from the blast-wave analogy are not in agreement with the experimental values.

COMPARISON TO OTHER METHODS

In the introduction, mention was made of various methods of calculation for surface pressures. These methods were used to compute surface pressures for one of the present test conditions, namely, $\lambda = 3$, $M_\infty = 5.7$, $\bar{\alpha} = 0$ (fig. 2). The values calculated are compared with measured pressures in figure 11. Pressures calculated by the modified Newtonian theory, equation (5), are noted to be lower than the measured values. Pressures were also calculated with a combination of Newtonian theory to the sonic point ($\alpha = 46^\circ$, $x/d = 0.06$) followed by Prandtl-Meyer expansion (without attempt to match pressure gradients), and these values are noted to be appreciably lower than the data. The application of inviscid sharp-wedge (oblique shock-wave) theory based on local surface inclination is noted in figure 11 to be lower than the measured values. (The angle of surface inclination at $x/d = 0.3$ is about 24° for this ellipse.) The linear method of reference 4 was also used to calculate pressures for these conditions. The corresponding curve is noted on figure 11 to be lower than the data points on the afterbody and to match the data at values of x/d less than about 0.8. This linear method is not seriously in error for this set of data. However, the method is limited, as previously mentioned, because the inviscid wedge theory is used for reference conditions at angle of attack. The present method which is, in part, based on local conditions at the boundary-layer edge is noted to predict the measured pressures over the range of x/d of figure 11 with better accuracy than any of the other methods discussed.

CONCLUDING REMARKS

A study was made of the effect of profile curvature on the hypersonic flow field over blunt plates. A method of calculating surface pressures was developed utilizing a combination of viscous and inviscid hypersonic parameters. Surface pressures were measured over the elliptic leading edge of blunted plates at a Mach number of 5.7 and free-stream Reynolds number per inch of 19,000.

The method developed herein was found to predict to engineering accuracy, the measured surface pressures obtained here and in other similar investigations. The applicability of the method was found to extend over a range of Mach number from 4 to 13.3, profiles of elliptic axis ratio of 1 to 8, Reynolds number of leading edges from 6,600 to 129,000, and in air and helium test gas. The surface inclinations extended over a range of angles from about 35° to 0° for elliptic profiles, and from 70° to 0° for circular profiles. Application of this method, however, is shown herein to require accurate assessment of the effect of the detached bow shock wave.

Ames Research Center
National Aeronautics and Space Administration
Moffett Field, Calif., May 21, 1959

APPENDIX A

THE PLANE BLAST WAVE

From the similarity assumptions utilized in the blast-wave theory (refs. 8 and 9) the pressure in the flow behind the shock wave is assumed to be given by

$$\frac{p}{p_\infty} = \frac{(dR/dt)^2}{a_\infty^2} f\left(\frac{r}{R}\right) \tag{A1}$$

In the above equation a_∞ is the sound speed in undisturbed air, (dR/dt) is the shock-wave velocity, and $f(r/R)$ is a function of location of a point between the blast source and the resultant shock wave and equal to about 0.45 on the body surface (ref. 8). The following relation was also obtained in the analysis of the blast wave for a planar source,

$$R^{1/2}\left(\frac{dR}{dt}\right) = \left(\frac{E_o}{\rho_\infty J}\right)^{1/2} \tag{A2}$$

where J is obtained from reference 8. For the plane wave and constant energy flow, the value of J is constant and equal to 1.2 for air and approximately 0.6 for helium. If the energy E_o (contained in unit width of the transverse flow field) is assumed in the analogy of the plane blast wave to the hypersonic flow over a planar body to be given by the pressure drag of the leading edge, then

$$E_o = C_D \frac{1}{2} \rho_\infty u_\infty^2 \frac{d}{2} \tag{A3}$$

From equations (A3) and (A2) the following is obtained

$$R^{1/2}\left(\frac{dR}{dt}\right) = u_\infty \sqrt{\frac{C_D d}{4J}} \tag{A4}$$

The velocity of the shock wave is obtained from equation (A4) as

$$\left(\frac{dR}{dt}\right)^2 = \frac{u_\infty{}^2 C_D d}{4JR} \tag{A5}$$

Thus the pressure in the flow field behind the shock wave is

$$\frac{p}{p_\infty} = \left[\frac{f(r/R)}{4J}\right] \frac{C_D M_\infty{}^2}{R/d} \tag{A6}$$

If equation (A4) is integrated, the following relation is obtained

$$R = \left(\frac{3}{2} u_\infty \sqrt{\frac{C_D d}{4J}}\right)^{2/3} t^{2/3} \tag{A7}$$

In the analogy of the plane blast wave to the hypersonic flow over a blunt planar body the time t is identified with the velocity u_∞ of the body and the distance x as follows

$$t = \frac{x+\Delta}{u_\infty} \tag{A8}$$

Thus equation (A7) when combined with (A8) becomes

$$R = \left(\frac{3}{2} u_\infty \sqrt{\frac{C_D d}{4J}}\right)^{2/3} \frac{(x+\Delta)^{2/3}}{(u_\infty)^{2/3}} \tag{A9}$$

If one divides both sides of equation (A9) by d, and rearranges factors, the shock-wave shape will be given by

$$\frac{R}{d} = K_1 (C_D)^{1/3} \left(\frac{x+\Delta}{d}\right)^{2/3} \tag{A10}$$

where

$$K_1 = \left(\frac{3}{4\sqrt{J}}\right)^{2/3}$$

The calculated value of K_1 is obtained as 0.78 for air and 0.975 for helium.

If equations (A6) and (A10) are combined, the pressure may be expressed as follows

$$\frac{p}{p_\infty} = \left[\frac{f(r/R)}{4JK_1}\right] \frac{(C_D)^{2/3} M_\infty^2}{(x+\Delta/d)^{2/3}} \tag{A11}$$

When equation (A11) is compared to equation (6) of the text, it is noted that the following relationship exists between the constant B of the blast-wave pressure equation and the constant K_1 of the shock-wave shape equation

$$BC_\gamma = \frac{f(r/R)}{4JK_1} \tag{A12}$$

For conditions of constant energy flow with planar symmetry, the value of B is calculated from equation (A12) to be 1.07 for air and 1.14 for helium.

REFERENCES

1. Penland, Jim A.: Aerodynamic Characteristics of a Circular Cylinder at Mach Number 6.86 and Angles of Attack Up to 90°. NACA TN 3861, 1957. (Supersedes NACA RM L54A14)

2. Creager, Marcus O.: Effects of Leading-Edge Blunting on the Local Heat Transfer and Pressure Distributions Over Flat Plates in Supersonic Flow. NACA TN 4142, 1957.

3. Bertram, Mitchell H., and Henderson, Arthur, Jr.: Effects of Boundary Layer Displacement and Leading-Edge Bluntness on Pressure Distribution, Skin Friction, and Heat Transfer of Bodies at Hypersonic Speeds. NACA TN 4301, 1958.

4. Creager, Marcus O.: Effect of Leading-Edge Sweep and Surface Inclination on the Hypersonic Flow Field Over a Blunt Flat Plate. NASA MEMO 12-26-58A, 1959.

5. Bogdonoff, S. M., and Vas, I. E.: Preliminary Study of the Flow Over a Blunt Flat Plate at Various Angles of Attack at M = 13.3. Part II: Study of an Elliptical Leading Edge. Bell Report No. D143-978-005, ASTIA AD-1131-079, ARDC-TR-56-41, Oct. 1, 1956.

6. Tamaki, Fumio, and Kim, Chul-Soo: Studies on the Hypersonic Flow Using a Double-Diaphragm Shock Tube. Jour. Phys. Soc. Japan, vol. 12, no. 5, May 1957, pp. 550-555.

7. Hammitt, Andrew G.: The Hypersonic Viscous Effect on a Flat Plate With a Finite Leading Edge. Aero. Eng. Lab. Rep. No. 378, Princeton Univ., March 1957.

8. Rogers, M. H.: Similarity Flows Behind Strong Shock Waves. Quart. Jour. Mech. and Appl. Math., vol. XI, pt. 4, Nov. 1958, pp. 411-422.

9. Sakurai, Akira: On the Propagation and Structure of the Blast Wave, I. Jour. Phys. Soc. Japan, vol. 8, no. 5, Sept. - Oct. 1953, pp. 662-669.

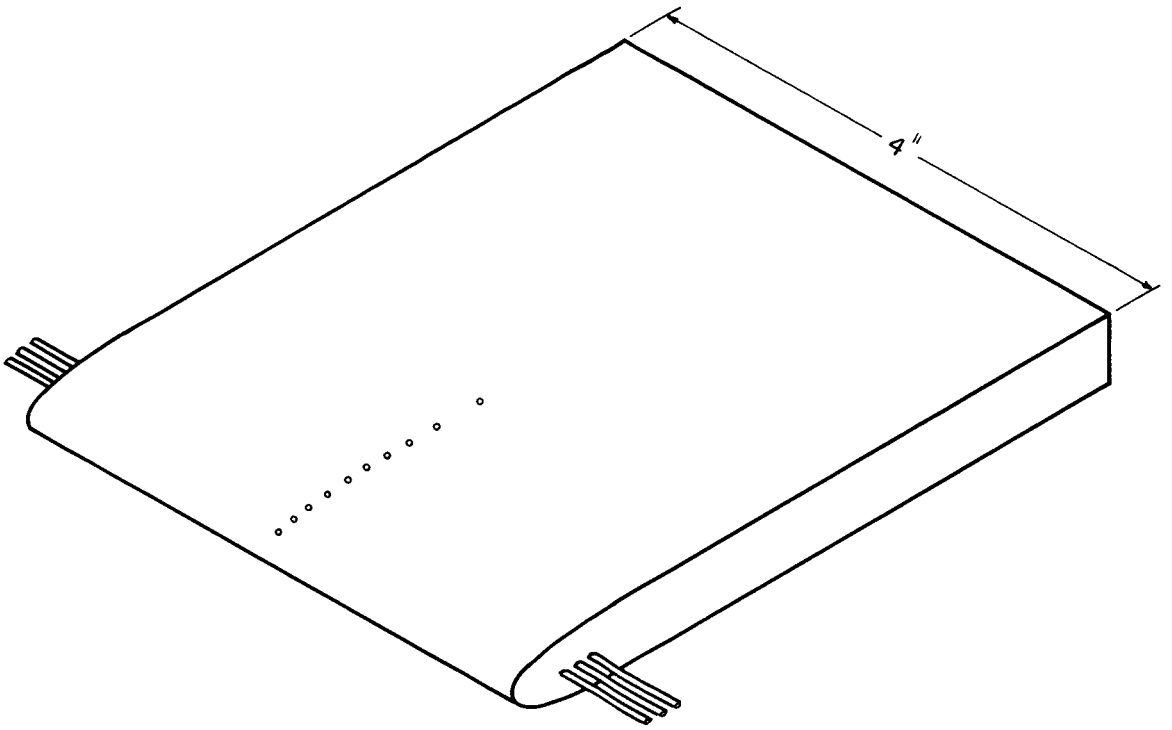

(a) Isometric view.

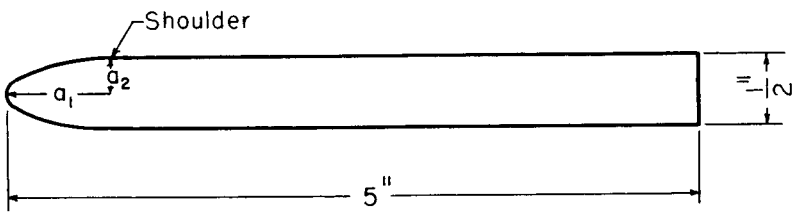

(b) Side view.

Figure 1.- Test body.

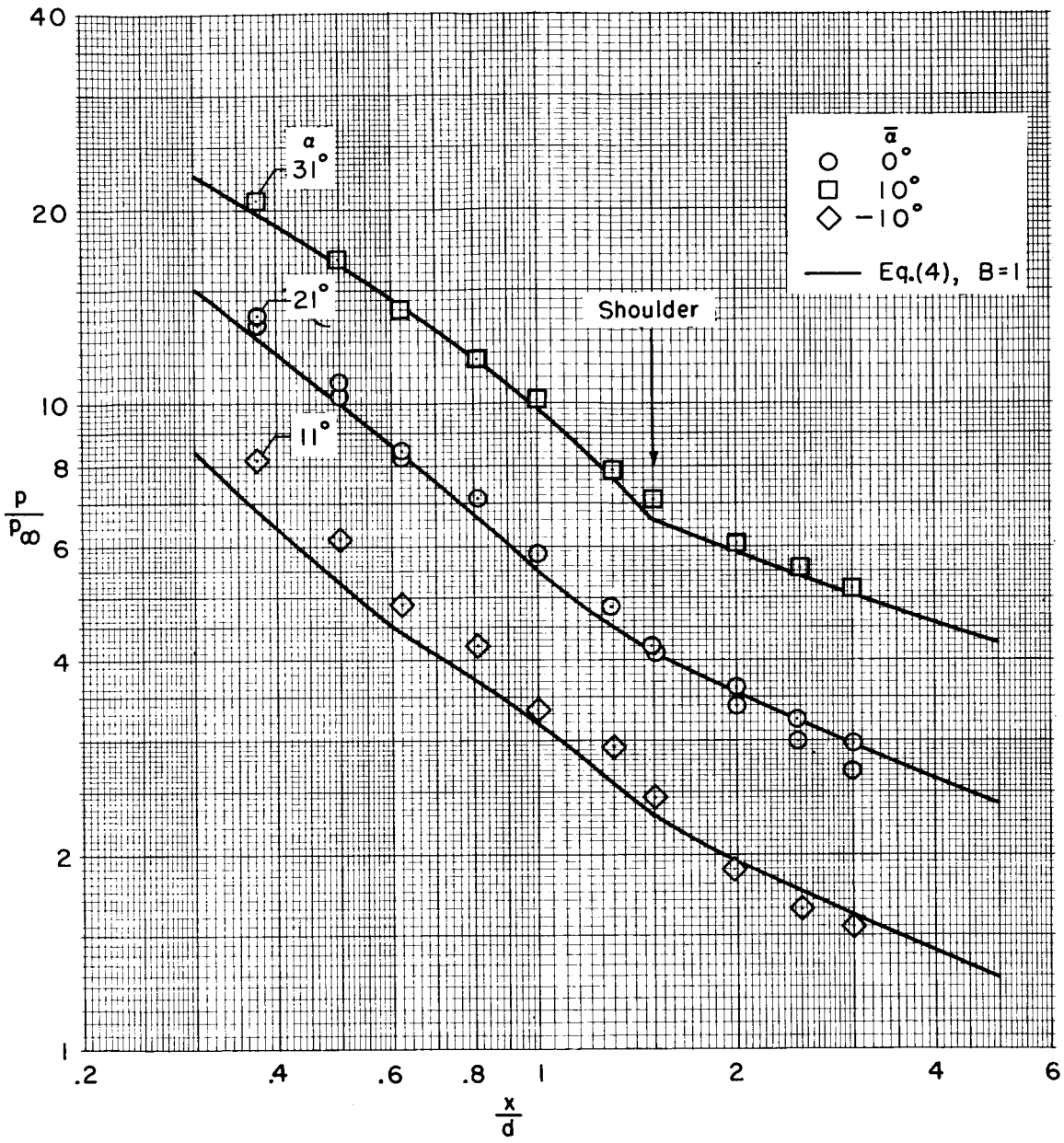

Figure 2.- Variation of surface pressure with chordwise distance for a blunt plate; $M_\infty = 5.7$, $Re_{\infty d} = 9{,}720$, $\lambda = 3$, air.

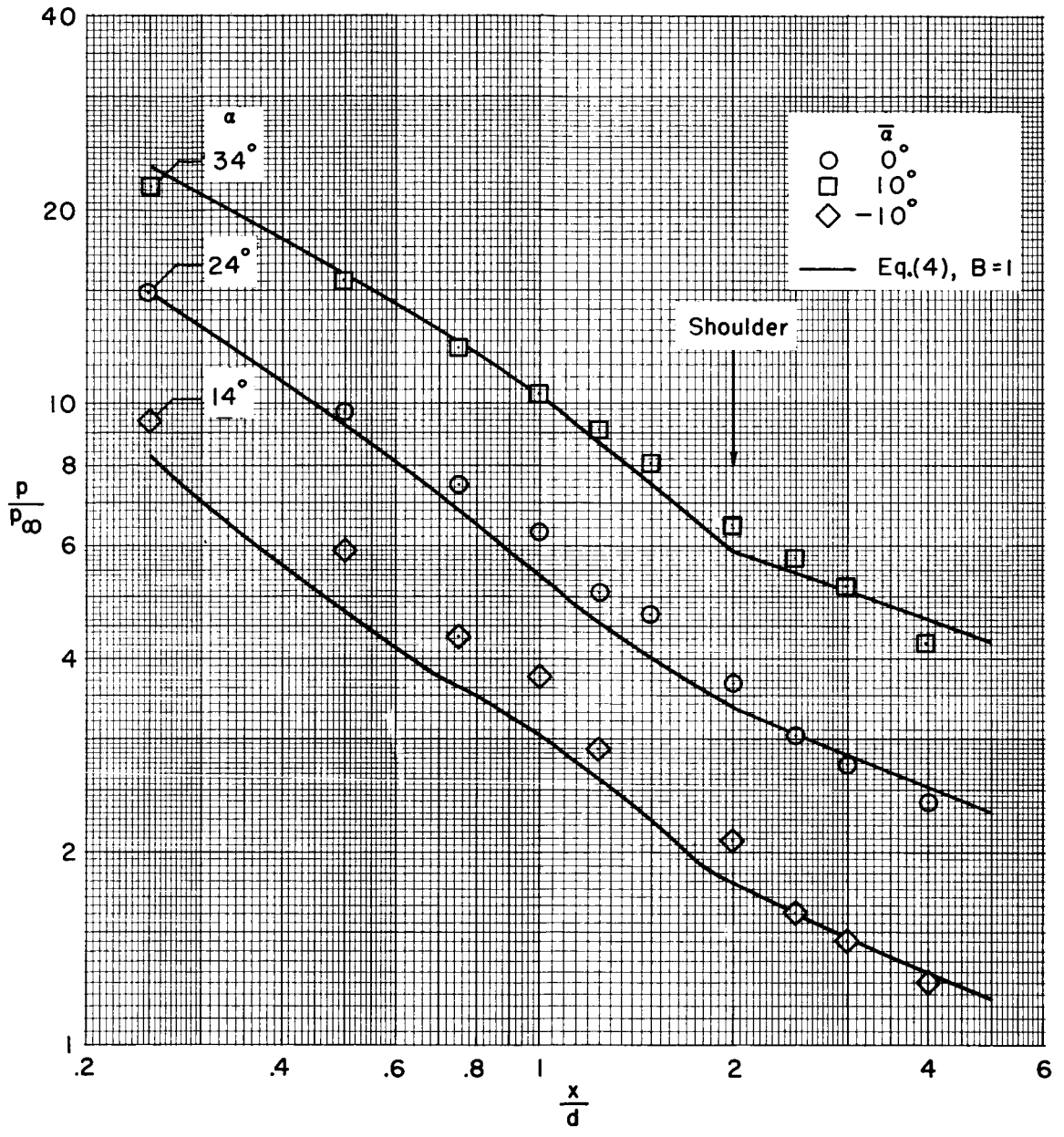

Figure 3.- Variation of surface pressure with chordwise distance for a blunt plate; $M_\infty = 5.7$, $Re_{\infty d} = 9{,}720$, $\lambda = 4$, air.

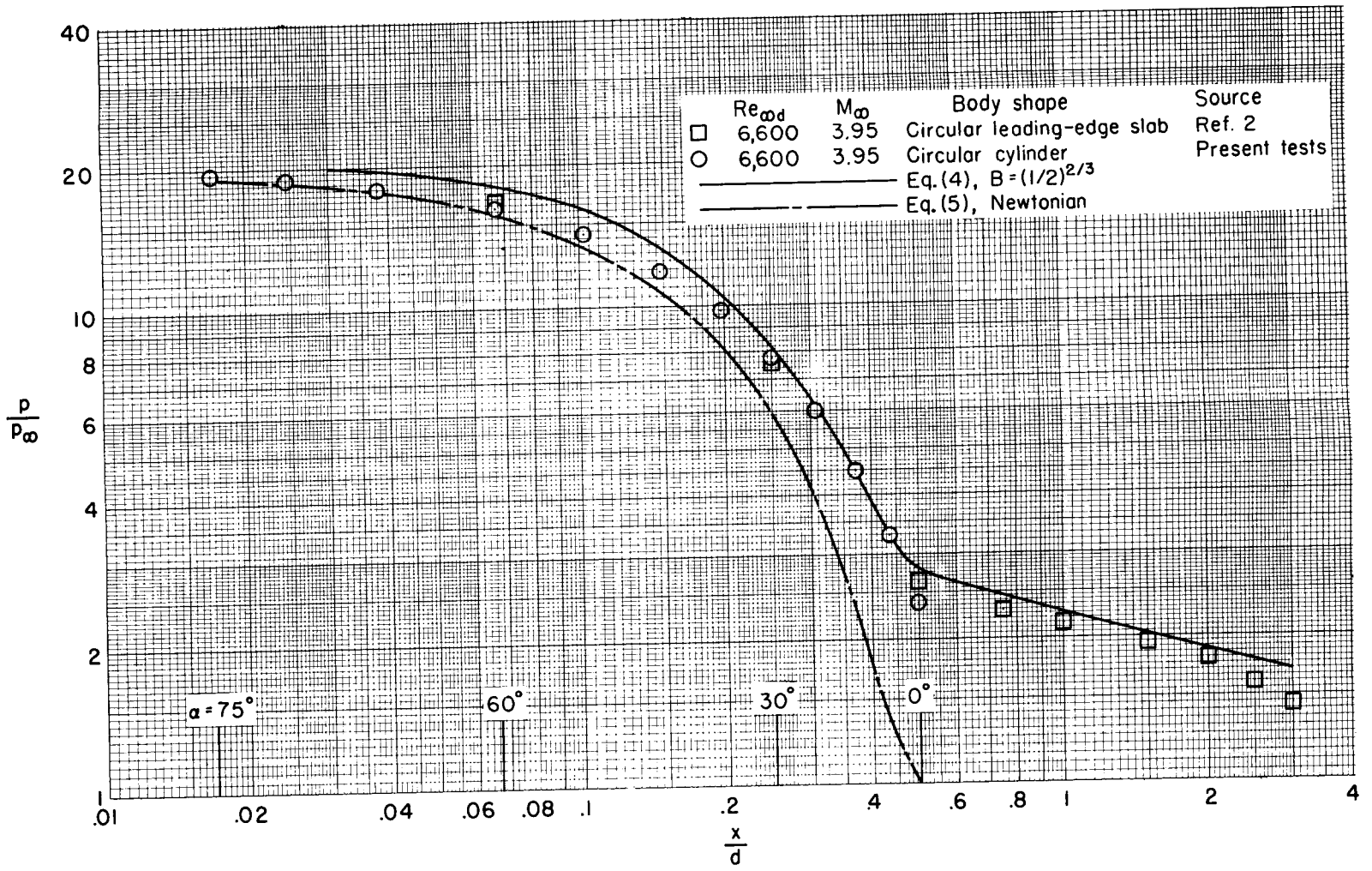

Figure 4.- Variation of surface pressures with chordwise distance for a blunt plate with a circular leading edge; $\lambda = 1$, $\bar{\alpha} = 0^{\circ}$, $\gamma = 1.4$.

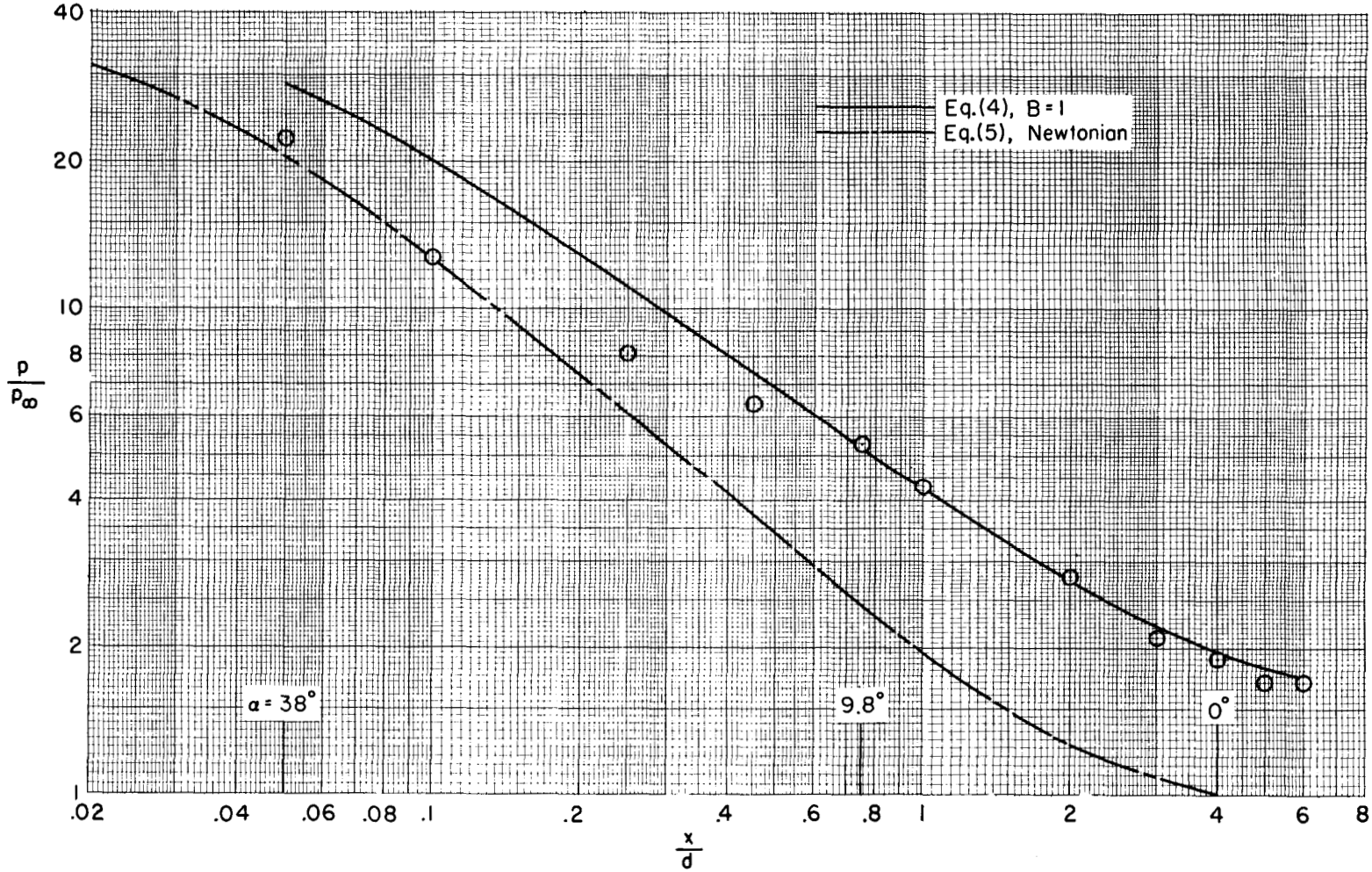

Figure 5.- Variation of surface pressures with chordwise distance for a blunt plate; $M_\infty = 6.4$, $Re_{\infty d} = 1.08 \times 10^5$, $\lambda = 8$, $\bar{\alpha} = 0^\circ$, air, reference 6.

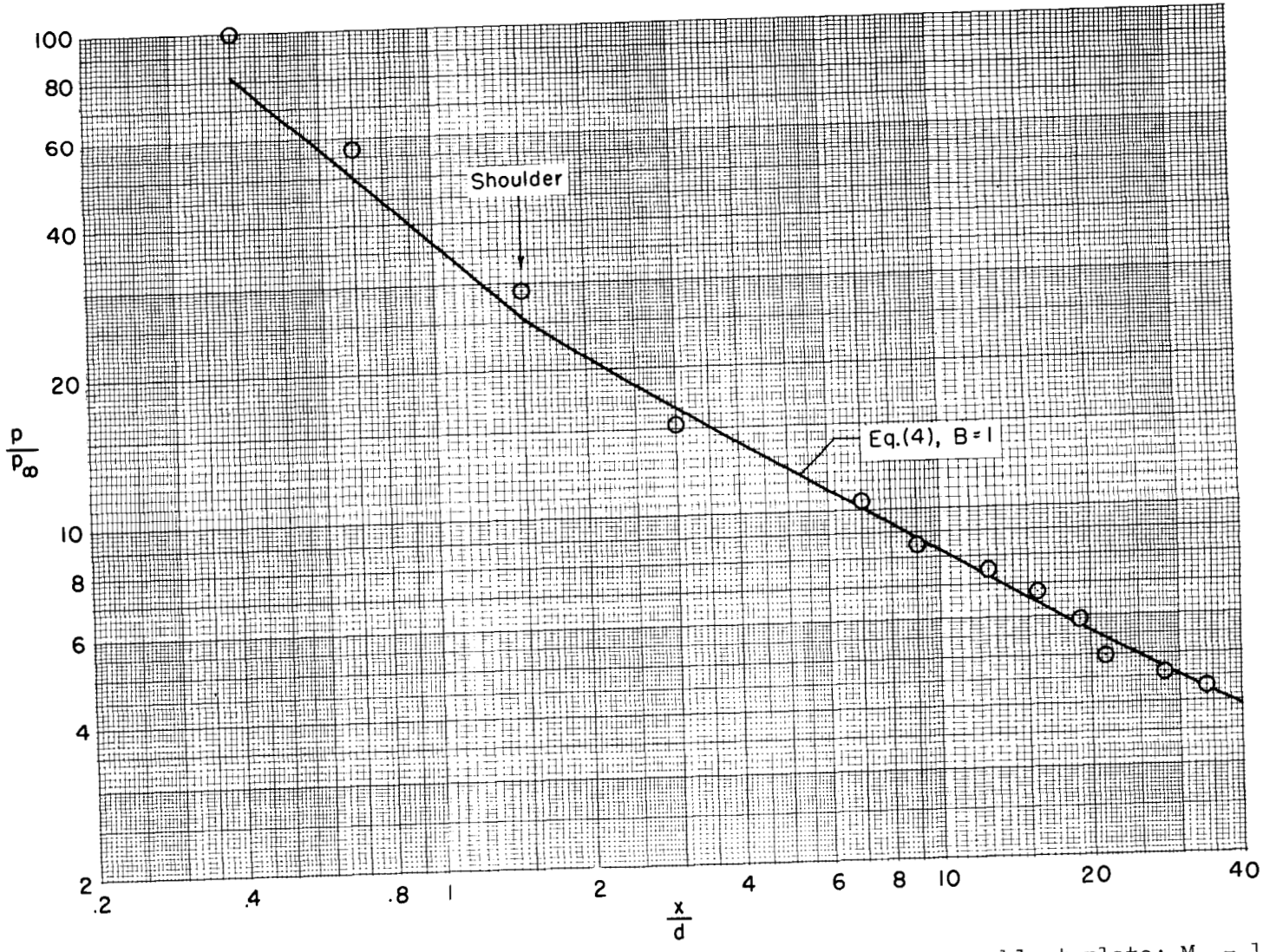

Figure 6.- Variation of surface pressures with chordwise distance for a blunt plate; $M_\infty = 13.3$, $Re_{\infty d} = 37{,}300$, $\lambda = 3$, $\bar{\alpha} = 0^\circ$, helium, reference 5.

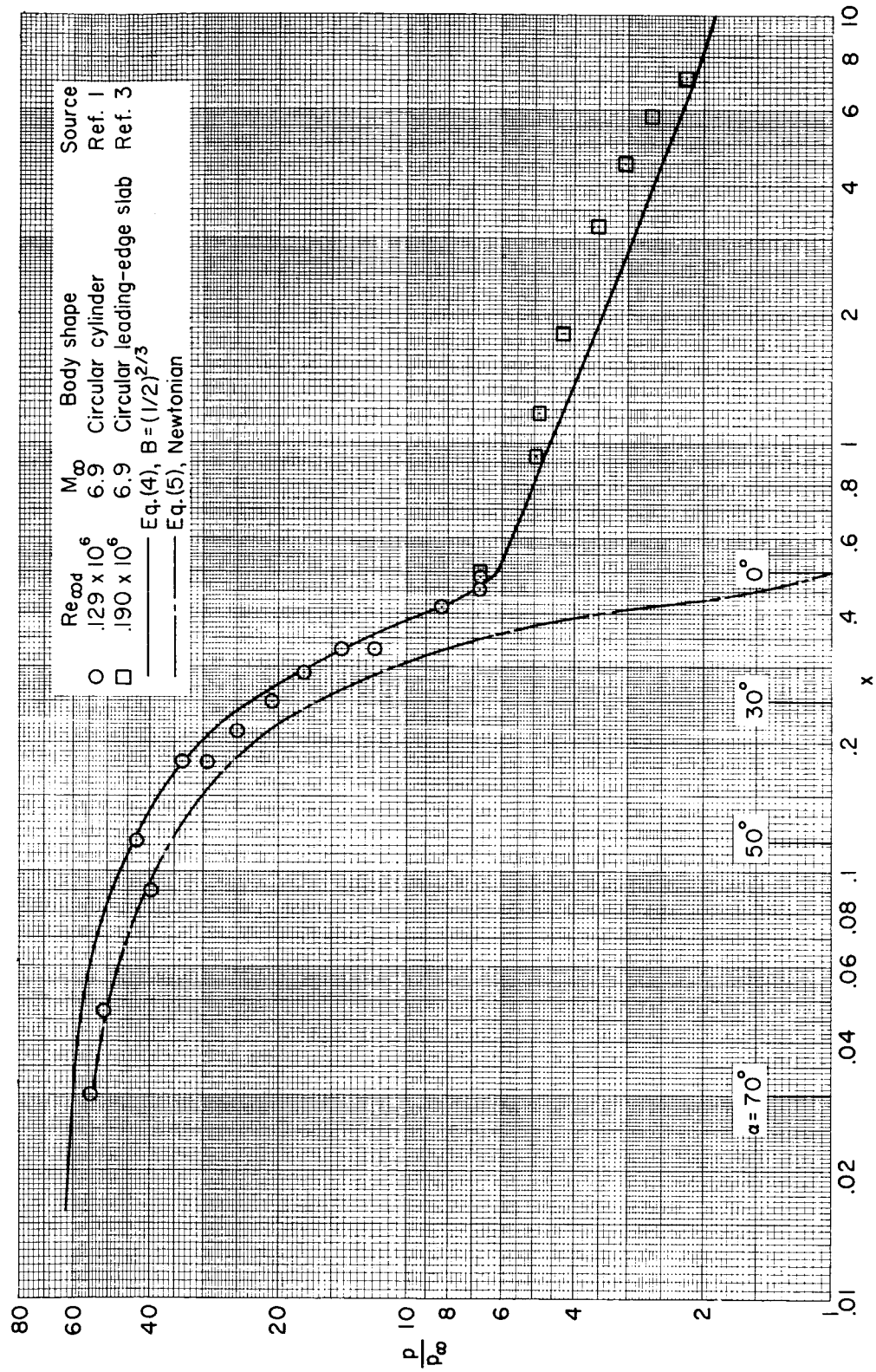

Figure 7.- Variation of surface pressures with chordwise distance for a blunt plate with a circular leading edge; $\lambda = 1$, air, $\bar{\alpha} = 0^\circ$.

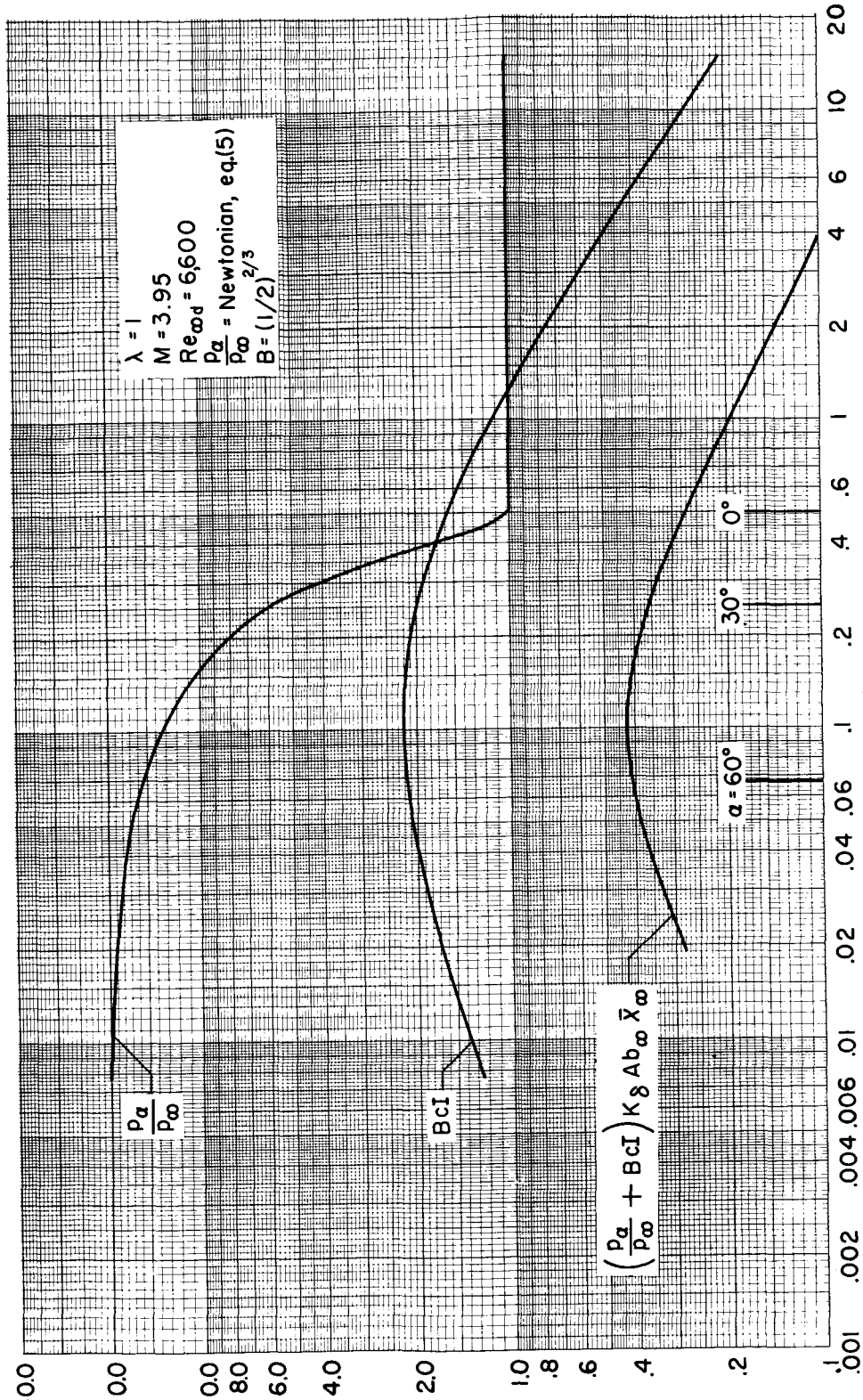

Figure 8.- Comparison of various terms of equation (4).

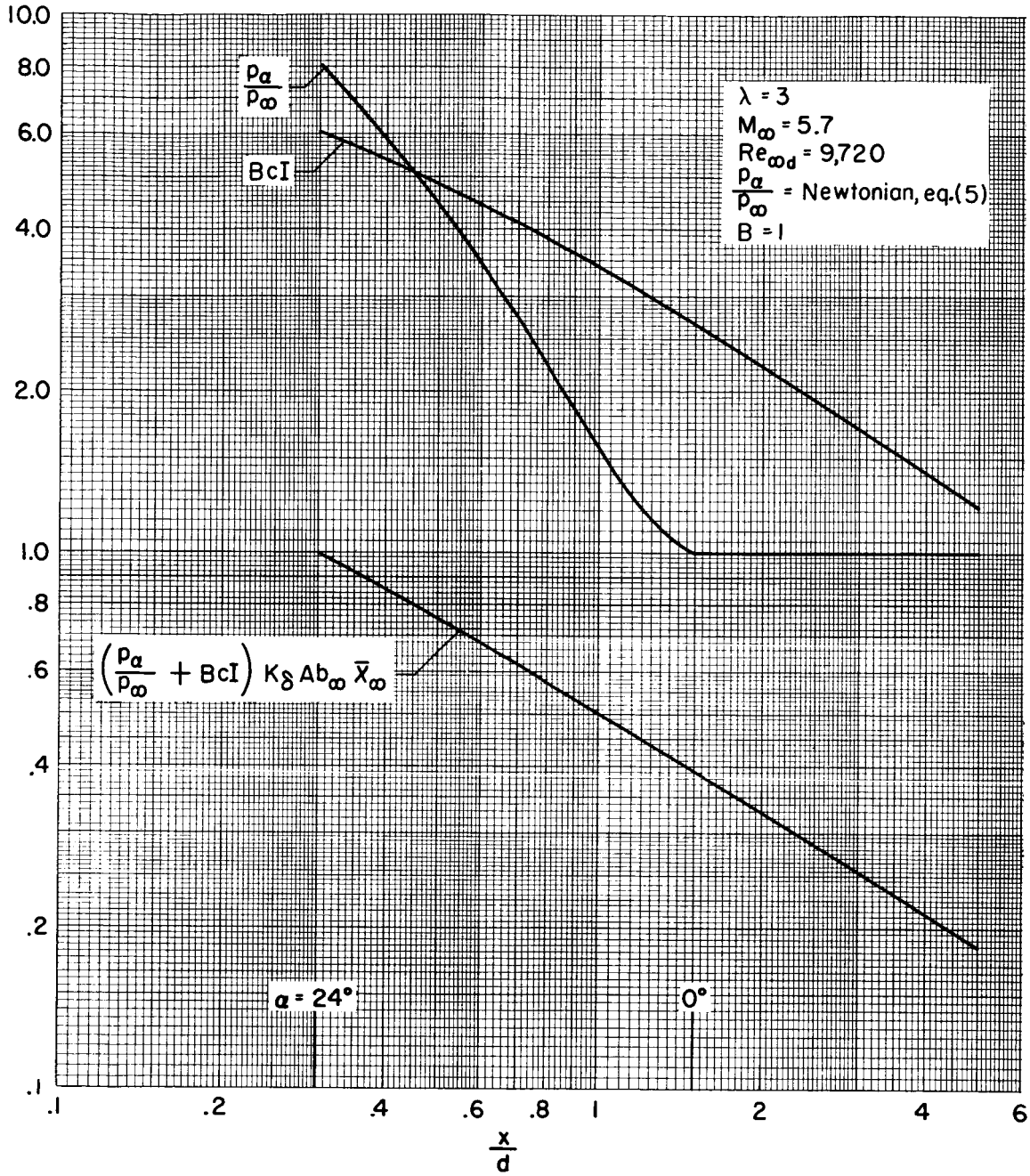

Figure 9.- Comparison of various terms of equation (4).

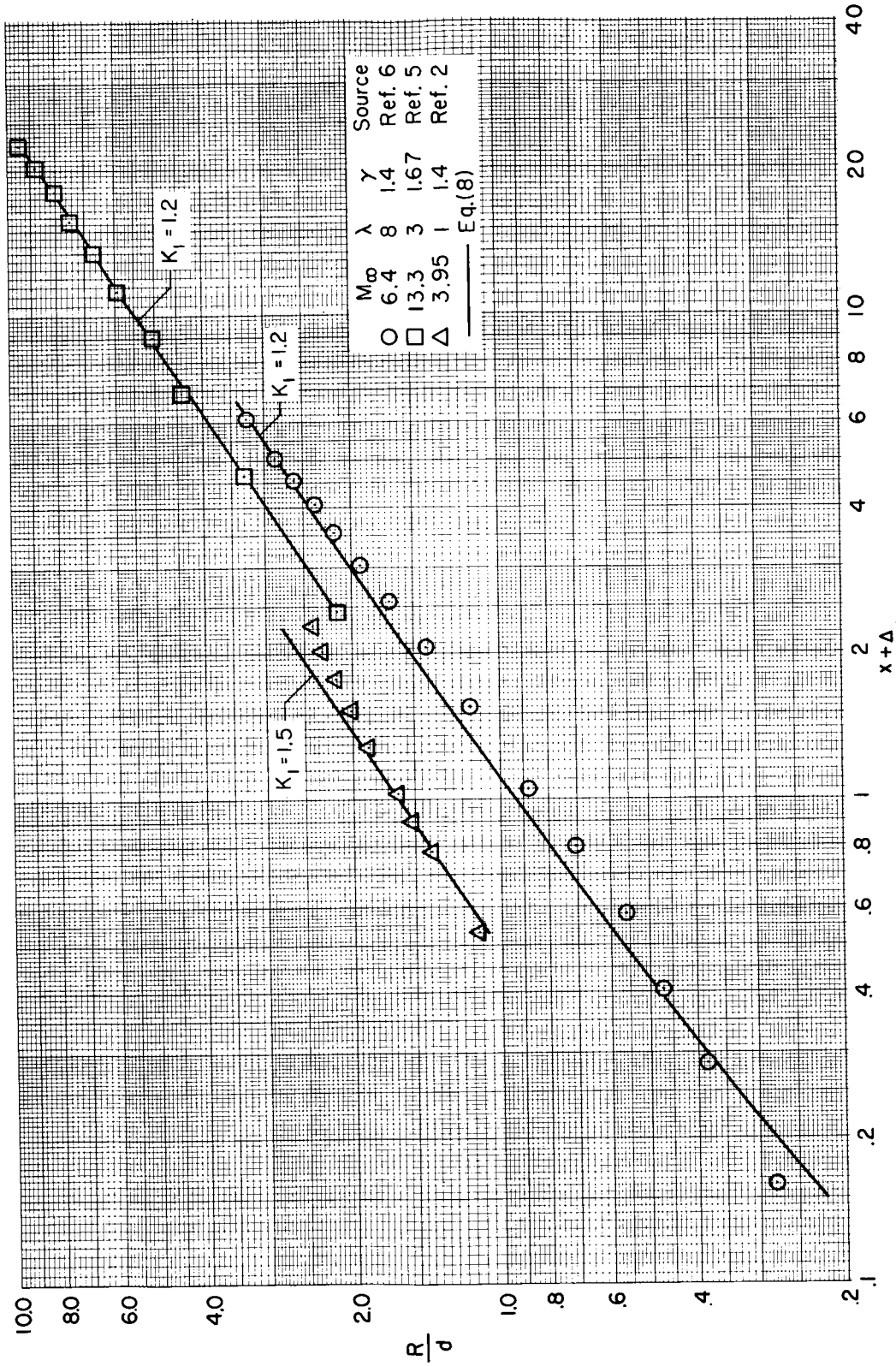

Figure 10.- Variation of shock-wave location with distance.

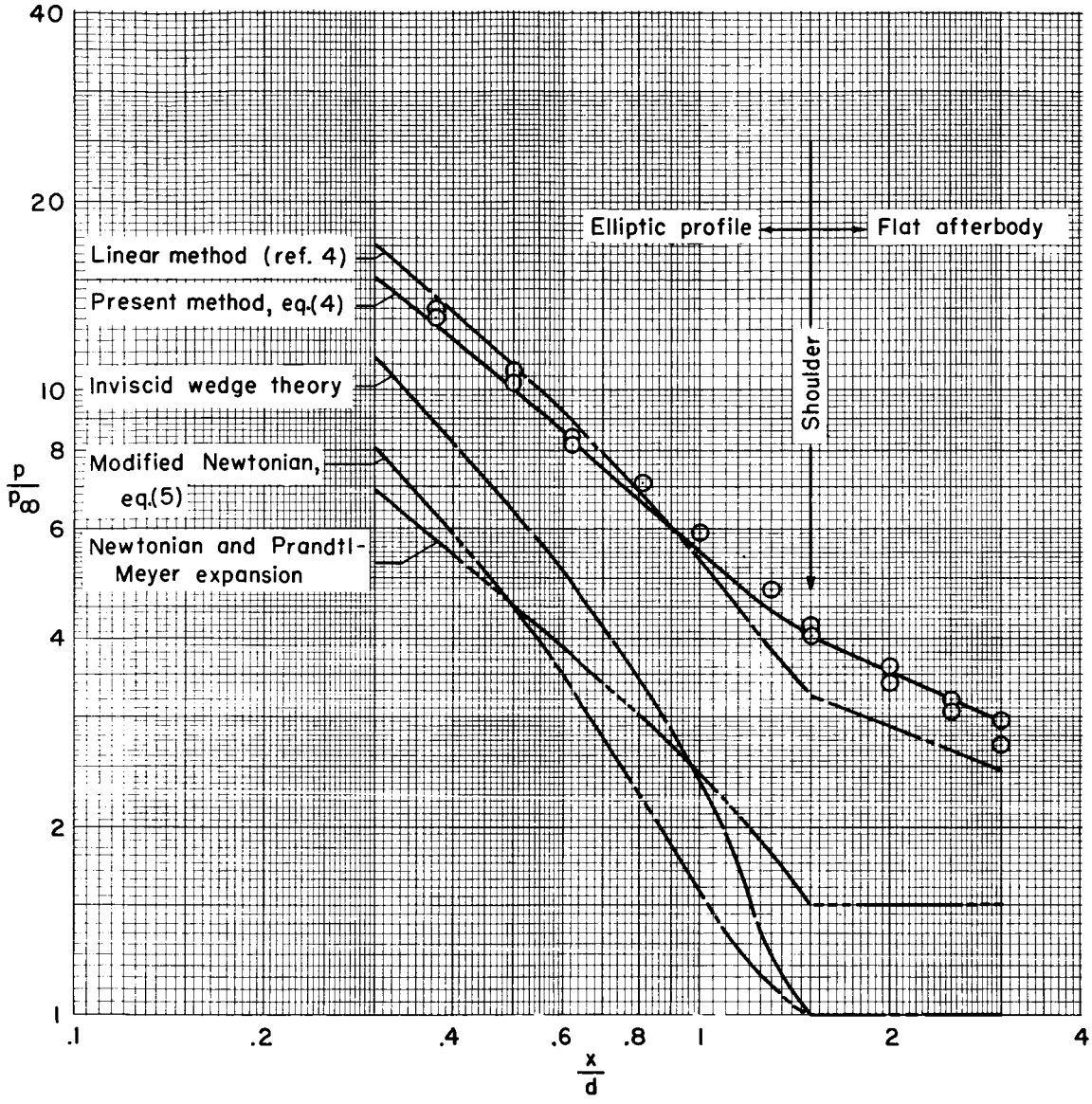

Figure 11.- Comparison of various methods of calculation to measurements for $M_\infty = 5.7$, $Re_{\infty d} = 9{,}720$, $\bar{\alpha} = 0^\circ$, $\lambda = 3$.